Acoustically Responsive Polydopamine Nanodroplets: A Novel Theranostic Agent

Christophoros Mannaris[1*], Chuanxu Yang[2], Dario Carugo[1,4], Joshua Owen[1], Jeong Yu Lee[1], Sandra Nwokeoha[1], Anjali Seth,[1], Boon Mian Teo[1,2,3*]

[1]Institute of Biomedical Engineering, Old Road Campus Research Building, University of Oxford, Oxford OX3 7DQ, UK
[2]Key Laboratory of Colloid and Interface Chemistry, Ministry of Education, Shandong University, Jinan, 250100, China
[3]School of Chemistry, Clayton Campus, Monash University Victoria, 3800, Australia
[4] Mechatronics and Bioengineering Science research groups, Faculty of Engineering and the Environment, University of Southampton, Southampton, UK
Email address: christophoros.mannaris@eng.ox.ac.uk, boonmian.teo@monash.edu

Keywords: ((ultrasound, Polydopamine, nanodroplets, acoustic droplet vaporization,))

Ultrasound-induced cavitation has been used as a tool of enhancing extravasation and tissue penetration of anticancer agents in tumours. Initiating cavitation in tissue however, requires high acoustic intensities that are neither safe nor easy to achieve with current clinical systems. The use of cavitation nuclei can however lower the acoustic intensities required to initiate cavitation and the resulting bio-effects *in situ*. Microbubbles, solid gas-trapping nanoparticles, and phase shift nanodroplets are some examples in a growing list of proposed cavitation nuclei. Besides the ability to lower the cavitation threshold, stability, long circulation times, biocompatibility and biodegradability, are some of the desirable characteristics that a clinically applicable cavitation agent should possess. In this study, we present a novel formulation of ultrasound-triggered phase transition sub-micrometer sized nanodroplets (~400 nm) stabilised with a biocompatible polymer, polydopamine (PDA). PDA offers some important benefits: (1) facile fabrication, as dopamine monomers are directly polymerised on the nanodroplets, (2) high polymer biocompatibility, and (3) ease of functionalisation with other molecules such as drugs or targeting species. We demonstrate that the acoustic intensities required to initiate

inertial cavitation can all be achieved with existing clinical ultrasound systems. Cell viability and haemolysis studies show that nanodroplets are biocompatible. Our results demonstrate the great potential of PDA nanodroplets as an acoustically active nanodevice, which is highly valuable for biomedical applications including drug delivery and treatment monitoring.

1. Introduction

Effective delivery of therapeutics to tumour sites is often hindered by poor drug solubility, rapid drug clearance, and harmful side effects.[1] Research into particles offering spatially and temporally sustained drug delivery, which can also target specific tumor sites, enhance uptake efficiency and boost bioavailability of therapeutic agents, has flourished in recent years.[2] Such delivery systems can respond to either endogenous signals such as enzymes [3-5], pH [6-9] and redox [10, 11], or exogenous signals such as light [12-14], magnetic fields, [15] and acoustic energy [16].

Ultrasound has gained popularity as a mechanical trigger in the treatment of cancer and cardiovascular diseases due to its non-invasive nature and its ability to penetrate deep within biological tissues. Furthermore, ultrasound can combine imaging and drug delivery to achieve *in situ* treatment monitoring[17]. Ultrasound responsive agents typically exploit cavitation to promote drug release and/or enhance the extravasation, penetration, and distribution of anticancer compounds at tumour sites[18],[19]. These cavitation-inducing agents may consist of pre-existing gas pockets, or liquid emulsions that phase transition to produce bubbles. At low acoustic pressure amplitudes, microbubbles exhibit stable volumetric oscillations, known as non-inertial cavitation. These are characterised by acoustic emissions containing harmonics and subharmonics of the driving ultrasound frequency which are exploited in contrast enhanced diagnostic imaging[20]. At higher acoustic pressures, microbubbles rapidly expand and violently collapse, a process known as inertial cavitation (IC)[21] and whose acoustic signatures are composed mainly of broadband emissions. Cavitation events can produce a range of

physical phenomena such as microstreaming, shockwaves, and liquid microjets that in turn give rise to biological effects[22] such as enhanced drug extravasation and tissue penetration.[23, 24] In addition, the acoustic emissions from cavitating bubbles can be detected outside the body and enable real time monitoring of the therapeutic process[25, 26] .

Although microbubbles are the gold standard in diagnostic ultrasound imaging, they have several disadvantages as drug delivery vehicles; they have short circulation times, they are rapidly destroyed upon ultrasound exposure[27], and their large size (2-10 μm) relative to the vessel size restricts them to the vasculature. In order to permeate the compromised vasculature within a tumour via the enhanced permeability and retention (EPR) effect,[28] much smaller particles are required. Consequently, liquid perfluorocarbon (PFC) nanodroplets that vaporise to form bubbles upon ultrasound exposure (termed acoustic droplet vaporisation or ADV) have been explored as an alternative agent. ADV was pioneered by Correas and Quay in 1996 and their therapeutic potential was firstly reported by Apfel[29] and Kripfgans *et al*.[30]

Nanodroplets have been shown to exhibit superior *in vivo* stability and circulation time compared to microbubbles, and much greater potential to extravasate into tumour tissues[31-33]. The stability of nanodroplets depends on their size, shell composition and thickness and more importantly, the PFC boiling point.[34] For an ideal spherical bubble with a thin shell having a surface tension σ, and a radius r, the internal pressure (P_{in}) is equal to the external pressure (P_{out}) increased by the Laplace pressure term ($2\sigma/r$). Nanodroplets typically remain stable under physiological conditions as the boiling point of perfluorohexane (PFH) is 57 °C at standard atmospheric pressure with a vaporization enthalpy of 34 kJ/mol,[35, 36]. When exposed to ultrasound, however, vaporisation can be induced due to the decreased pressure imposed on the droplet during the rarefaction phase of acoustic waves.[34]

Chemotherapy drugs have been successfully incorporated into nanodroplets and delivered to cells *in vitro*.[37-40] Recent studies have also indicated that nanodroplets can function as a DNA carrier for cellular gene transfection, and the successful release of microRNA and small

interfering RNA upon ultrasound exposure has been demonstrated[41-44]. Incorporation of multiple types of drugs, particularly bio-active agents and targeting species, however can represent a significant challenge as it requires modification of the nanodroplet coating.

Due to its versatility and excellent biocompatibility, polydopamine (PDA) has been utilised as a coating material for colloidal particles of diverse surface composition for various biomedical applications.[32, 45] Dopamine undergoes consecutive oxidation, intramolecular cyclisation, and oligomerisation/self-assembly in slightly alkaline conditions, leading to highly adhesive PDA. This approach, originally inspired by the inherent adhesive properties of mussels, was recently introduced and several papers have demonstrated the facile fabrication of a range of PDA coated substrates.[32] Recent studies have reported the formation of PDA films on electrodes for bio-sensing,[46] PDA-stabilized poly(l-lysine)/hyaluronic acid multilayered films,[47] and multifunctional PDA-coated carbon nanotubes.[48] It has also been demonstrated that PDA-coated gold nanoparticles exhibit long term superior stability *in vivo*.[49] Although PDA has been utilised in several biomedical applications, to the best of our knowledge, acoustically active PDA agents have not yet been engineered. The aim of this study is to engineer and characterise acoustically responsive PDA-based perfluorocarbon nanodroplets (Figure 1). Specifically, we report on the assembly of PDA shelled nanodroplets by spontaneous oxidative interfacial polymerisation of a dopamine solution onto pluronic f127 stabilised emulsions to form stable nanodroplets. We demonstrated that the droplets are stable in physiological conditions, and investigated the acoustic vaporisation threshold and onset of cavitation activity of such constructs for ultrasound mediated drug delivery. We showed that PDA nanodroplets exhibit negligible toxicity towards MCF7 breast cancer cells and red blood cells, which is of great importance for their application in drug delivery. Our findings support the potential utility of PDA in the engineering of acoustically active agents for ultrasound theranostics.

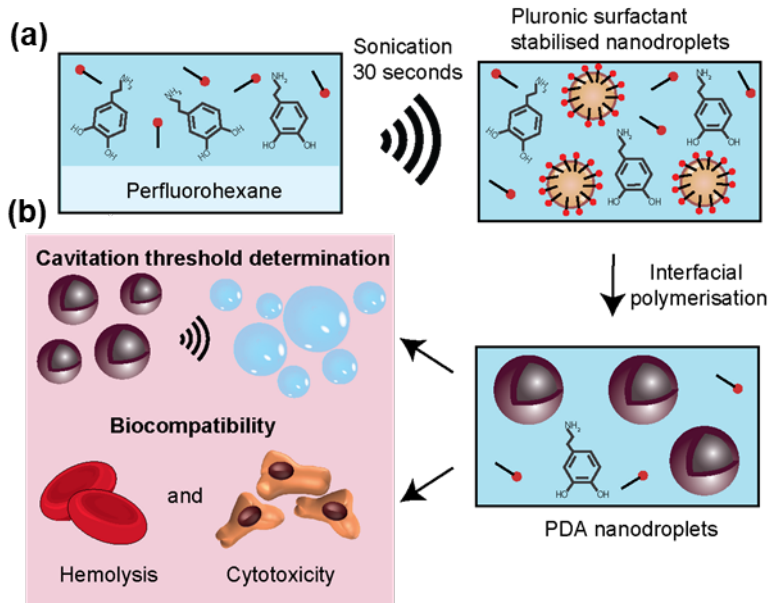

Figure 1: a) Fabrication of acoustically responsive PDA nanodroplets via interfacial polymerization and b) determination of the cavitation threshold and biocompatibility of the liquid PFH nanodroplets.

2. Materials and Methods

2.1 Materials

All chemicals were purchased from commercial suppliers and used without further purification. Dopamine hydrochloride, pluronic f127, tris(hydroxymethyl)aminomethane (TRIS), copper (I) sulfate (Cu_2SO_4) and doxorubicin hydrochloride (Dox) were purchased from Sigma-Aldrich, UK. Perfluorohexane (PFH) was obtained from Apollo Scientific (Cheshire, UK). Fetal bovine serum (FBS), phosphate buffered saline (PBS) and Dulbecco's Modified Eagle's Medium (DMEM) were purchased from Life Technologies Ltd (Paisley, UK). MTS assay was purchased from Promega UK, Southampton, UK. Deionized (DI) water was used in all experiments, and degassed DI water was used in experiments involving ultrasound.

2.2 Methods

2.2.1 Fabrication of PDA nanodroplets

Dopamine hydrochloride (1 mg) and pluronic f127 (1 mg) were dissolved in 3 ml of 10 mM TRIS buffer (pH 8.5). 0.8 vol % of Cu_2SO_4 and 50 µL of PFH were added to the mixture and

sonicated in ice for 30 seconds at 6 W with a 20 kHz ultrasonic probe. The emulsion was then allowed to stir for 60 minutes. The colour of the mixture changed from pale yellow to dark brown as the dopamine polymerization progressed. Following this, the resulting PDA coated nanodroplets were washed 3 times with water via centrifugation (500 g, 10 min) to ensure complete removal of the unreacted dopamine and redispersed in PBS (pH 7.4).

2.2.2 Characterisation of PDA nanodroplets

The hydrodynamic diameter of the prepared nanodroplets was measured using a zeta-potential & particle size analyzer (ZEN3600, Malvern Instruments, Worcestershire, UK) from 3 separate samples, at both 20 °C and 37 °C. The size of the nanodroplets were determined using transmission electron microscopy (TEM, FEI Tecnai 12, USA). A 10 μL sample of nanodroplets dispersed in aqueous solution (2 mg/mL) was deposited on a Formvar/carbon supported copper grid and stained with 2% uranyl acetate. The grid was dried in air for 1 h at room temperature and observed using TEM. The concentration of nanodroplets dispersed in PBS was measured by Nanoparticle Tracking Analysis (NanoSight, Wiltshire, UK). FT-IR spectra were obtained on a Bruker Tensor 27 system using attenuated total reflectance (ATR) sampling accessories.

2.2.3 Acoustic response characterization of PDA nanodroplets

A multi-layered acoustic resonator comprised of an optically transparent chamber was used to characterize the phase transition efficiency of different PDA nanodroplets upon ultrasound exposure. Details of this device have been published elsewhere[38]. Briefly, the acoustic resonator comprises the following: a piezoelectric transducer, a carrier layer that couples the acoustic energy to the other components of the device, a fluidic layer with nanodroplets in suspension, and a reflector component that reflects the acoustic energy back into the device. The experimentally measured resonance frequency for the device was 1.85 MHz, in good agreement with computational predictions. The transducer was driven with a continuous wave at a fixed voltage of 40 V peak-to-peak. The ensuing peak rarefactional pressure in the

chamber was 265 kPa, measured with a calibrated fiber-optic hydrophone (Precision Acoustics, Dorchester, UK). 500 µL of the nanodroplet suspension was injected into the device, which was then covered with a glass slide. The device was then mounted onto the stage of Nikon TI Eclipse fluorescent microscope (Nikon UK Ltd, Kingston upon Thames, UK) and the solutions containing the droplets were exposed to ultrasound for different time intervals at room temperature. It should be noted that this experimental set up only provides a qualitative readout of nanodroplet phase transition upon ultrasound exposure, and is designed for high-throughput screening of different droplet formulations.

The acoustic vaporization threshold for the PDA nanodroplets was also measured by detection of acoustic emissions in a flow phantom. The flow phantom was composed of 1.25% (w/v) low melting point ultrapure agarose gel (Invitrogen, Carlsbad, CA, USA) with an embedded 1 mm channel that was created by heating and cooling process. A clear and acoustically transparent Mylar film was used to isolate the gel from the surrounding water and allow free propagation of ultrasonic waves, while a low-pulsatility peristaltic pump (Minipulse Evolution, Gilson, Middleton, WI, USA) was used to inject the droplet solution at a constant flow rate of (0.2 mL/min). A schematic cartoon of the experimental setup used is shown in Figure 2.

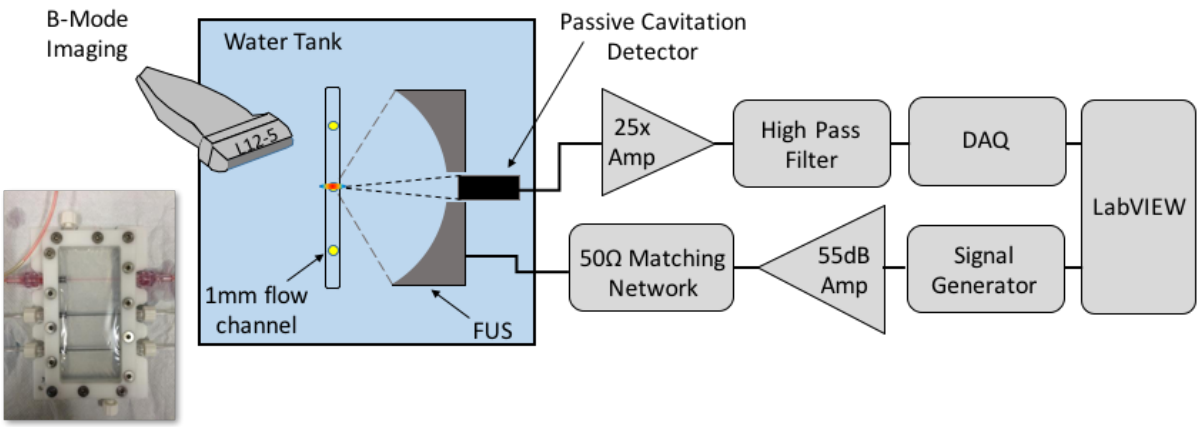

Figure 2. Schematic cartoon of the experimental setup for detection of acoustic emissions from nanodroplets following ADV. The inset photograph shows the flow phantom in plan view.

A 0.5 MHz ultrasound transducer (Sonic Concepts, Bothell, WA, USA) was focused on 1-mm channel through which a flow of the droplets suspension was established. A 7.5 MHz single element transducer (V320, Panametrics, Olympus, Waltham, MA, USA) was coaxially and confocally aligned with the 0.5 MHz transducer. The pressure output from the 0.5 MHz transducer was calibrated using a 0.4-mm-diameter needle hydrophone (ONDA 1056, Onda Corporation). Both transducers were controlled using a software custom-written in the graphical programming language Labview (National Instruments, Austin, TX, USA). Acoustic emissions arising from ADV and subsequent cavitation were detected by the 7.5 MHz transducer and filtered using a 5 MHz high pass filter (FILT-HP5-A, Allen Avionics), amplified 25 times with a low noise amplifier (Stanford Research Systems, SR445A) and recorded with a 14-bit PCI Oscilloscope device (PCI-5122, National Instruments, Austin, TX, USA) at a rate of 100 MHz. The high-pass filter was ultilised to reject strong reflections from the flow phantom at the fundamental frequency (and harmonics due to non-linear propagation). The pressure threshold required to initiate ADV was determined by exposing the flow of droplets to 200-cycle pulses from the 0.5 MHz transducer, the pressure amplitude of which was gradually increased. The pulse repetition frequency was chosen as to allow the ultrasound focus to be refreshed with droplets for each exposure and the duty cycle was kept

below 5% to minimize any thermal effects. The vaporization threshold was defined as the pressure needed for an increase in electrical signal variance received by the PCD that was >6 standard deviations above baseline electrical noise. Each time this occurred, a cavitation event was counted and the probability of cavitation was calculated (300 bursts were transmitted at each pressure step).

A Zonare Z.One (Mindray, Shenzhen, China) clinical ultrasound scanner was used for real-time imaging during the experiment. The imaging allowed monitoring of the integrity of the channel to detect possible leaks, and make sure the flow was uniform and did not contain any exogenous air bubbles. Harmonic imaging was used at a low mechanical index to prevent any interference of the imaging with the therapeutic pulse.

2.2.6 Cell culturing

MCF7 breast cancer cells were cultured in RPMI medium supplemented with 10% fetal bovine serum (FBS) and 1% penicillin-streptomycin at 37 °C in 5% CO_2 and 100% humidity. The cells were seeded in Ibidi cell dishes (Thistle Scientific Ltd, Glasgow, UK) at a density of 5×10^4 cells per dish and grown in DMEM at 37 °C for 24 h. After overnight incubation, 100 µL fresh medium was exchanged and the cells were incubated for another 48 h before analysis with MTS assay.

Cytotoxicity assay. The cytotoxicity of the PDA droplets was investigated by a MTS assay (Molecular Probes, Life Technologies) according to manufacturer's protocol. Cells were seeded in a 96-well plate at a density of 5×10^4/well in 100 µL medium for 24 h. The medium was then replaced with 100 µL of fresh medium containing PDA droplets at different number concentrations (0 - 5×10^8 nanodroplets). After 24 h incubation, the cells were rinsed with PBS and treated with MTS reagent (10% in medium) for 2 h. A plate reader (FLUOstar OPTIMA, Moritex BioScience) at an excitation wavelength of 540 nm and emission wavelength of 590 nm was used to analyse the samples.

2.2.7 Hemolysis assay

1 mL of blood was diluted with 2 mL of PBS (pH 7.4), centrifuged at 8000 rpm for 10 minutes, and the supernatant was discarded. The purified red blood cells (RBC) were resuspended in 10 mL PBS. Subsequently, 200 μL of RBC suspension was incubated with various particle concentrations (0-5×10^8) of PDA nanodroplets under gentle shaking and was kept at room temperature for 3 hours. The resultant suspension (200 μL) was incubated in PBS and H_2O (800 μL) serving as negative and positive controls, respectively. The samples were subsequently centrifuged for 12 000 rpm for 5 minutes and the absorbance values of the supernatants at 540 nm were determined.

3. Results and Discussion

3.1 Fabrication and characterization of PDA nanodroplets

The size of PDA nanodroplets can be controlled via the dopamine interfacial polymerization time. As shown in Figure 3(a), there was a sharp increase in PDA film growth on pluronic F127 stabilised nanodroplets during the first 30 minutes, followed by a linear and slower PDA film growth from 60 minutes onwards. The chemical attributes of PDA droplets were investigated using Fourier transform infrared spectrometry (FTIR). The similar FTIR spectra of both pure PDA and PDA nanodroplets (Figure 3(b)) indicates successful coating of PDA on pluronic stabilized nanodroplets. The peaks at 1600 cm^{-1} are consistent with the indole or indoline structures, while the peak at approximately 3370 cm^{-1} is in accordance with the presence of hydroxyl structures. Figure 3(c) shows a representative transmission electron microscopy (TEM) image of PDA droplets; the white spots correspond to PFH surrounded by darker rings due to the uranyl acetate stained PDA shells.

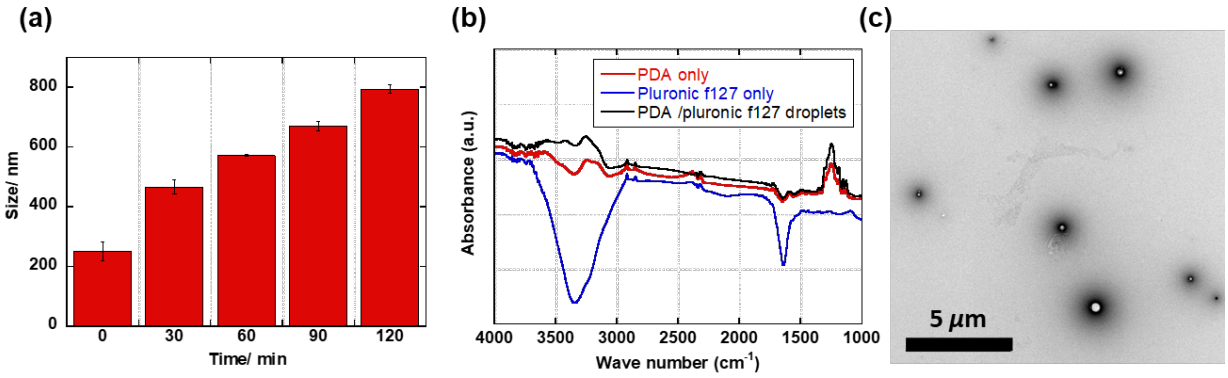

Figure 3: a) average size of PDA nanodroplets as a function of dopamine polymerization time, b) FTIR of pristine PDA(red line), pluronic-f127 (blue line) and PDA nanodroplets (black line), and c) TEM image of 60 min coated PDA nanodroplets.

3.2 Ultrasound triggered phase transition of nanodroplets

Vaporization of the droplets was observed by optical microscopy, within an acoustofluidic device developed in house.[50] Before ultrasound exposure, the nanodroplets sediment in water due to the higher relative density of the liquid perfluorohexane (PFH) core. Following exposure

to ultrasound[a], droplets vaporise to produce buoyant microbubbles (Figure 4). The shell of the microbubbles remain intact during the vaporisation process as shown in Figure S1, revealing that the PDA microbubbles are sufficiently robust as acoustically active agents.

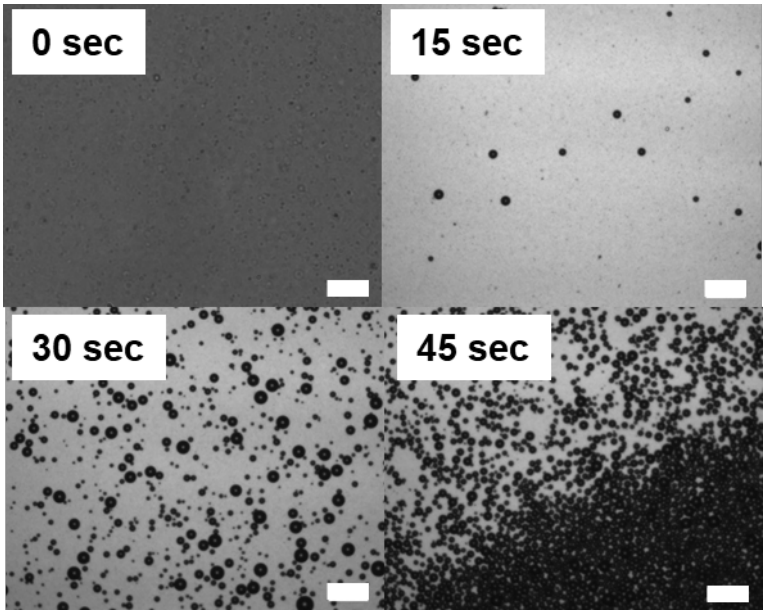

Figure 4: Optical images of PDA nanodroplets before and after 15, 30 and 45 seconds of ultrasound exposure (continuous wave, 1.8 MHz, 265 kPa). Scale bars are 200 μm.

3.3 Acoustic droplet vaporization and cavitation threshold under flow conditions

Due to their small size and similar impedance to tissue, liquid nanodroplets are invisible to diagnostic ultrasound. When vaporized however, the newly formed microbubbles can provide significant contrast to the surrounding tissue and can be imaged with a clinical scanner. Figure 5(a) shows an example of PDA nanodroplets flowing in an agarose tissue mimicking flow phantom while the in-situ pressure of the focused ultrasound (FUS) is varied from below to above their vaporization threshold.

[a] It should be noted that the droplet solution was static and continuous wave ultrasound was used in this setup. Results for droplets under flow conditions and exposed to a more clinically relevant pulsed ultrasound exposure regime are presented below.

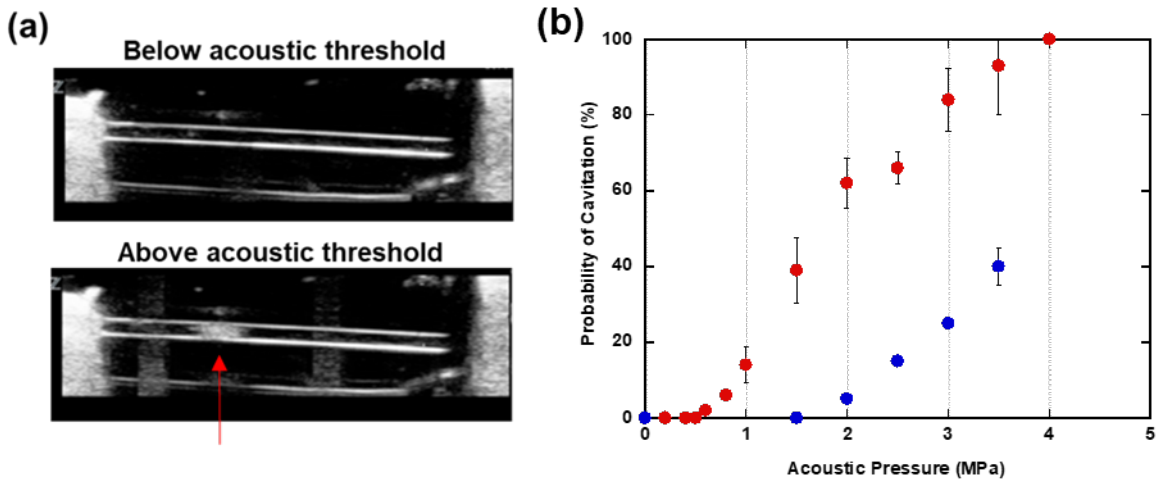

Figure 5: Harmonic imaging of PDA droplets in a vessel phantom exposed to 0.5 MHz FUS. Red arrow indicates direction of FUS (a) Top: When the acoustic pressure is below the vaporisation threshold droplets are in their liquid phase and cannot be detected via ultrasound imaging; bottom: When the pressure is increased above the vaporisation threshold, the resulting microbubbles can be clearly seen within the channel. b) Cavitation probability of flowing droplets at 0.5 MHz as a function of peak negative acoustic pressure.

The pressure threshold to initiate vaporisation and subsequent cavitation activity was determined by ramping 200-cycle FUS bursts continuously with small pressure increments under constant flow. There is a clear threshold at an acoustic peak negative pressure of 1 MPa, below which no phase transition occurs, while the probability of cavitation reaches 80% at 3 MPa.

3.3 Stability of PDA nanodroplets

Good colloidal stability is essential for successful application of nanomaterials *in vivo*.[51] We therefore evaluated the stability of PDA droplets in PBS and 10% serum (at 37 °C) and monitored changes in droplet mean diameter, size dispersity, and volumetric concentration. Figure 6 shows the average droplet diameter, polydispersity index (PDI) and concentration as a function of time. There was no pronounced decrease in the size of droplets, no changes in the PDI and the concentration of droplets remained consistent throughout the tested days, indicating that PDA droplets are colloidally stable under physiological conditions. Notably, droplets

remained stable for several days at 37 °C, and can be kept at 4 °C for several months without apparent reduction in stability (data not shown).

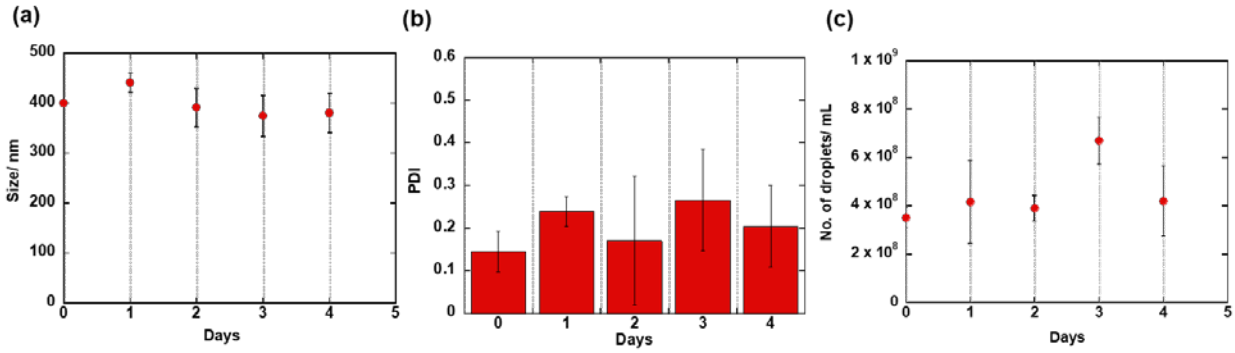

Figure 6: Stability of PDA nanodroplets as a function of time. (a) Droplet mean diameter, (b) polydispersity index and (c) number of droplets/ mL.

3.4 Biocompatibility of PDA nanodroplets

It is critical that drug carriers do not themselves induce cytotoxic effects. Drug carrier toxicity has been shown to be concentration dependent[52, 53]. To determine the appropriate dose of PDA nanodroplets that will not elicit toxicity effects on MCF7 breast cancer cells, the 3-(4,5-dimethylthiazol-2-yl)-5-(3-carboxymethoxyphenyl)-2-(4-sulfophenyl)-2H-tetrazolium (MTS) assay was employed. Figure 7 shows cell viability after 48 h of incubation with different concentrations of PDA nanodroplets. A cell viability of over 75% was maintained upon increasing the number nanodroplets concentration from 3×10^7 to 5×10^8. This concentration range is within the reported range for drug delivery applications.[54] The results indicated that an appropriate dose of PDA nanodroplets should be carefully selected for drug delivery purposes.

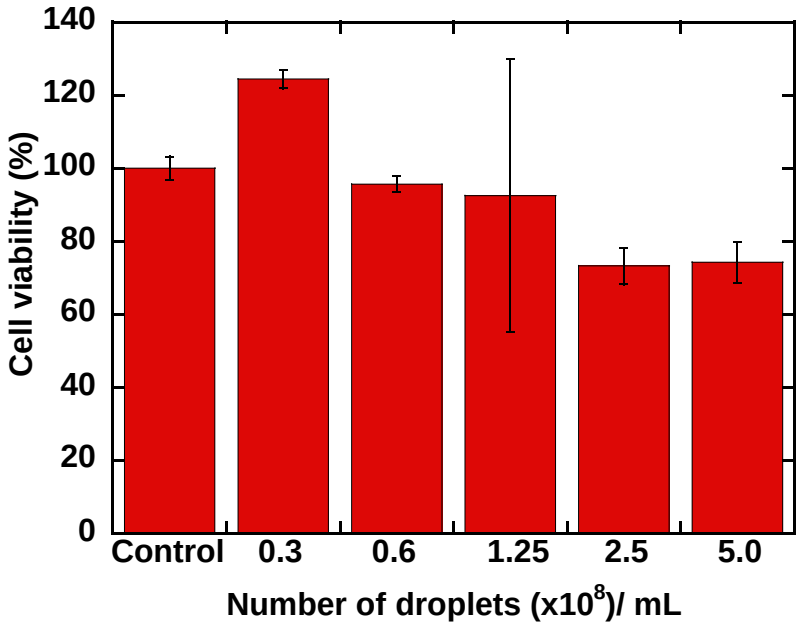

Figure 7: MTS assay of PDA droplets on MCF7 cells incubated with increasing nanodroplet concentration 24 hours at 37 °C with 5% CO_2. The cell viability values were normalized to the untreated cells (control viability = 100%). The polymerization time used for PDA coating on the nanodroplets was 60 minutes.

Blood compatibility is another critical pre-requisite for clinical applications of nanomaterials, because their interaction with blood components in the circulatory system can result in significant toxicity to humans.[55] To further investigate the biocompatibility of PDA nanodroplets, a haemolysis assay was conducted. During the haemolysis assay, haemoglobin released into the solution is directly proportional to the haemolytic activity of the carrier, therefore the absorbance at 541 nm can be used to quantify the haemolytic activity. Figure 8 shows the haemolysis results for PDA nanodroplets at different concentrations. The photograph of RBCs samples after 3 hours exposure to different concentrations of nanodroplets is shown in Figure 7a. The incubation of the nanodroplets with RBCs revealed low haemolytic activity of nanodroplets, as there is no apparent red colour that would originate from the breaking of RBCs membrane. Quantitative analysis using UV-vis spectroscopy demonstrated that PDA nanodroplets had negligible haemolytic activity and optical images (Figure S2) of the RBCs after incubation with varying concentration of nanodroplets also revealed negligible haemolysis.

Results indicate that for the concentrations tested, PDA nanodroplets would be non-toxic towards erythrocytes after intravenous injection.

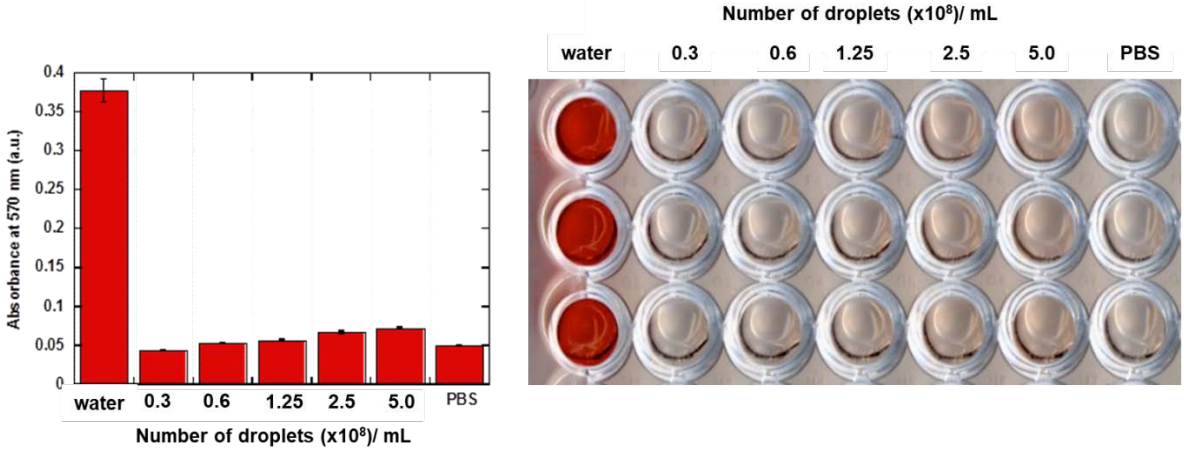

Figure 8: Haemolysis test on PDA nanodroplets following incubation of red blood cells with increasing nanodroplet concentration (original number concentration of nanodroplets: 1×10^8).

Conclusions

In summary, we have presented a new formulation of theranostic carrier based on PDA coated nanodroplets for ultrasound mediated drug delivery. These biocompatible PDA nanodroplets can be easily fabricated and well dispersed in saline solutions with high colloidal stability. Acoustic vaporization of the nanodroplets has been shown to occur at pressures as low as 1 MPa at 0.5 MHz, easily achievable with existing clinical ultrasound systems. Once vaporised, the resulting gas bubbles have also been shown to exhibit high contrast-to-tissue ratio thus allowing real-time imaging of the therapeutic process.

The nanodroplets showed no harmful side effects to red blood cells or MCF7 cells. Their sub-micron size (~400 nm) allows these nanodroplets to reach small capillaries and passively extravasate through the leaky tumour vasculature and, following cavitation, further enhance the penetration and distribution of the therapeutics. Investigation of using such droplets for ultrasound triggered combinatorial therapy is currently underway as well as toxicity and pharmacokinetic studies *in-vivo*.

Acknowledgement

BMT acknowledges the Danish Council for Independent Research, Technology and Production Sciences and Sapere Aude level 1 grant. The authors thank J Fisk and D Salisbury for manufacturing the phantom holders used in this work. In addition, the authors are grateful to the EPSRC for supporting this research through Grant No. EP/I021795/1 and Programme Grant No. EP/L024012/1 (OxCD3: OxfordCentre for Drug Delivery Devices).

References

1. Allen, T.M. and P.R. Cullis, *Drug Delivery Systems: Entering the Mainstream.* Science, 2004. **303**(5665): p. 1818.
2. Sahle, F.F., M. Gulfam, and T.L. Lowe, *Design strategies for physical-stimuli-responsive programmable nanotherapeutics.* Drug Discovery Today, 2018. **23**(5): p. 992-1006.
3. Hu, J., G. Zhang, and S. Liu, *Enzyme-responsive polymeric assemblies, nanoparticles and hydrogels.* Chemical Society Reviews, 2012. **41**(18): p. 5933-5949.
4. Hu, Q., P.S. Katti, and Z. Gu, *Enzyme-responsive nanomaterials for controlled drug delivery.* Nanoscale, 2014. **6**(21): p. 12273-12286.
5. Gu, Z., et al., *Glucose-Responsive Microgels Integrated with Enzyme Nanocapsules for Closed-Loop Insulin Delivery.* ACS Nano, 2013. **7**(8): p. 6758-6766.
6. Felber, A.E., M.-H. Dufresne, and J.-C. Leroux, *pH-sensitive vesicles, polymeric micelles, and nanospheres prepared with polycarboxylates.* Advanced Drug Delivery Reviews, 2012. **64**(11): p. 979-992.
7. Zhang, S., et al., *pH-responsive supramolecular polymer gel as an enteric elastomer for use in gastric devices.* Nature materials, 2015. **14**(10): p. 1065-1071.
8. Gao, W., J.M. Chan, and O.C. Farokhzad, *pH-Responsive Nanoparticles for Drug Delivery.* Molecular Pharmaceutics, 2010. **7**(6): p. 1913-1920.
9. Liu, J., et al., *pH-Sensitive nano-systems for drug delivery in cancer therapy.* Biotechnology Advances, 2014. **32**(4): p. 693-710.
10. McCarley, R.L., *Redox-Responsive Delivery Systems.* Annual Review of Analytical Chemistry, 2012. **5**(1): p. 391-411.
11. Luo, Z., et al., *Redox-Responsive Molecular Nanoreservoirs for Controlled Intracellular Anticancer Drug Delivery Based on Magnetic Nanoparticles.* Advanced Materials, 2012. **24**(3): p. 431-435.
12. Zhang, Y., et al., *Chain-Shattering Polymeric Therapeutics with On-Demand Drug-Release Capability.* Angewandte Chemie International Edition, 2013. **52**(25): p. 6435-6439.
13. Melancon, M.P., M. Zhou, and C. Li, *Cancer Theranostics with Near-Infrared Light-Activatable Multimodal Nanoparticles.* Accounts of Chemical Research, 2011. **44**(10): p. 947-956.
14. Rai, P., et al., *Development and Applications of Photo-triggered Theranostic Agents.* Advanced drug delivery reviews, 2010. **62**(11): p. 1094-1124.
15. Stanley, S.A., et al., *Radio-Wave Heating of Iron Oxide Nanoparticles Can Regulate Plasma Glucose in Mice.* Science (New York, N.Y.), 2012. **336**(6081): p. 604-608.

16. Qian, X., X. Han, and Y. Chen, *Insights into the unique functionality of inorganic micro/nanoparticles for versatile ultrasound theranostics.* Biomaterials, 2017. **142**: p. 13-30.
17. Kiessling, F., et al., *Recent Advances in Molecular, Multimodal and Theranostic Ultrasound Imaging.* Advanced drug delivery reviews, 2014. **0**: p. 15-27.
18. Coussios, C.C. and R.A. Roy, *Applications of Acoustics and Cavitation to Noninvasive Therapy and Drug Delivery.* Annual Review of Fluid Mechanics, 2008. **40**(1): p. 395-420.
19. Arvanitis, C.D., et al., *Cavitation-Enhanced Extravasation for Drug Delivery.* Ultrasound in Medicine and Biology. **37**(11): p. 1838-1852.
20. Tang, M.X., et al., *Quantitative contrast-enhanced ultrasound imaging: a review of sources of variability.* Interface Focus, 2011. **1**(4): p. 520-539.
21. Holland, C. and R. E. Apfel, *Thresholds for Transient Cavitation Produced by Pulsed Ultrasound in a Controlled Nuclei Environment.* Vol. 88. 1990. 2059-69.
22. Mitragotri, S., *Healing sound: the use of ultrasound in drug delivery and other therapeutic applications.* Nat Rev Drug Discov, 2005. **4**(3): p. 255-260.
23. Datta, S., et al., *CORRELATION OF CAVITATION WITH ULTRASOUND ENHANCEMENT OF THROMBOLYSIS.* Ultrasound in medicine & biology, 2006. **32**(8): p. 1257-1267.
24. Kooiman, K., et al., *Increasing the Endothelial Layer Permeability Through Ultrasound-Activated Microbubbles.* IEEE Transactions on Biomedical Engineering, 2010. **57**(1): p. 29-32.
25. Gyöngy, M. and C.-C. Coussios, *Passive cavitation mapping for localization and tracking of bubble dynamics.* The Journal of the Acoustical Society of America, 2010. **128**(4): p. EL175-EL180.
26. Coviello, C., et al., *Passive acoustic mapping utilizing optimal beamforming in ultrasound therapy monitoring.* The Journal of the Acoustical Society of America, 2015. **137**(5): p. 2573-2585.
27. Thapar, A., et al., *Dose-Dependent Artifact in the Far Wall of the Carotid Artery at Dynamic Contrast-enhanced US.* Radiology, 2012. **262**(2): p. 672-679.
28. Jain, R.K. and T. Stylianopoulos, *Delivering nanomedicine to solid tumors.* Nat Rev Clin Oncol, 2010. **7**(11): p. 653-664.
29. Apfel, R.E., *Activatable infusable dispersions containing drops of a superheated liquid for methods of therapy and diagnosis*. 1998, Google Patents.
30. Kripfgans, O.D., et al., *Acoustic droplet vaporization for therapeutic and diagnostic applications.* Ultrasound in Medicine and Biology. **26**(7): p. 1177-1189.
31. Rapoport, N., et al., *Ultrasound-Mediated Tumor Imaging and Nanotherapy using Drug Loaded, Block Copolymer Stabilized Perfluorocarbon Nanoemulsions.* Journal of controlled release : official journal of the Controlled Release Society, 2011. **153**(1): p. 4-15.
32. Liu, M., et al., *Recent developments in polydopamine: an emerging soft matter for surface modification and biomedical applications.* Nanoscale, 2016. **8**(38): p. 16819-16840.
33. Rapoport, N., et al., *Focused ultrasound-mediated drug delivery to pancreatic cancer in a mouse model.* Journal of Therapeutic Ultrasound, 2013. **1**(1): p. 11.
34. Sheeran, P.S., et al., *Design of ultrasonically-activatable nanoparticles using low boiling point perfluorocarbons.* Biomaterials, 2012. **33**(11): p. 3262-3269.
35. Matsunaga, T.O., et al., *Phase-Change Nanoparticles Using Highly Volatile Perfluorocarbons: Toward a Platform for Extravascular Ultrasound Imaging.* Theranostics, 2012. **2**(12): p. 1185-1198.

36. Hasty, D., et al., *Applications of Correlation Gas Chromatography and Transpiration Studies for the Evaluation of the Vaporization and Sublimation Enthalpies of Some Perfluorinated Hydrocarbons.* Journal of Chemical & Engineering Data, 2012. **57**(8): p. 2350-2359.
37. Dayton, P.A., et al., *Application of Ultrasound to Selectively Localize Nanodroplets for Targeted Imaging and Therapy.* Molecular Imaging, 2006. **5**(3): p. 7290.2006.00019.
38. Lee, J.Y., et al., *Nanoparticle-Loaded Protein–Polymer Nanodroplets for Improved Stability and Conversion Efficiency in Ultrasound Imaging and Drug Delivery.* Advanced Materials, 2015. **27**(37): p. 5484-5492.
39. Fabiilli, M.L., et al., *Delivery of Chlorambucil Using an Acoustically-Triggered Perfluoropentane Emulsion.* Ultrasound in Medicine & Biology, 2010. **36**(8): p. 1364-1375.
40. Zhou, H.-f., et al., *αvβ3-Targeted nanotherapy suppresses inflammatory arthritis in mice.* The FASEB Journal, 2009. **23**(9): p. 2978-2985.
41. Gao, D., et al., *Ultrasound-Triggered Phase-Transition Cationic Nanodroplets for Enhanced Gene Delivery.* ACS Applied Materials & Interfaces, 2015. **7**(24): p. 13524-13537.
42. Lee, J.Y., et al., *Ultrasound-Enhanced siRNA Delivery Using Magnetic Nanoparticle-Loaded Chitosan-Deoxycholic Acid Nanodroplets.* Advanced Healthcare Materials, 2017. **6**(8): p. 1601246-n/a.
43. Burgess, M.T. and T.M. Porter, *Acoustic Cavitation-Mediated Delivery of Small Interfering Ribonucleic Acids with Phase-Shift Nano-Emulsions.* Ultrasound in Medicine and Biology. **41**(8): p. 2191-2201.
44. Paproski, R.J., et al., *RNA Biomarker Release with Ultrasound and Phase-Change Nanodroplets.* Ultrasound in Medicine and Biology. **40**(8): p. 1847-1856.
45. Liebscher, J., et al., *Structure of Polydopamine: A Never-Ending Story?* Langmuir, 2013. **29**(33): p. 10539-10548.
46. Loget, G., et al., *Electrodeposition of Polydopamine Thin Films for DNA Patterning and Microarrays.* Analytical Chemistry, 2013. **85**(21): p. 9991-9995.
47. Jourdainne, L., et al., *Dynamics of Poly(l-lysine) in Hyaluronic Acid/Poly(l-lysine) Multilayer Films Studied by Fluorescence Recovery after Pattern Photobleaching.* Langmuir, 2008. **24**(15): p. 7842-7847.
48. Song, Y., et al., *Bioinspired Polydopamine (PDA) Chemistry Meets Ordered Mesoporous Carbons (OMCs): A Benign Surface Modification Strategy for Versatile Functionalization.* Chemistry of Materials, 2016. **28**(14): p. 5013-5021.
49. Choi, C.K.K., et al., *A Gold@Polydopamine Core–Shell Nanoprobe for Long-Term Intracellular Detection of MicroRNAs in Differentiating Stem Cells.* Journal of the American Chemical Society, 2015. **137**(23): p. 7337-7346.
50. Pereno, V., et al., *Layered acoustofluidic resonators for the simultaneous optical and acoustic characterisation of cavitation dynamics, microstreaming, and biological effects.* Biomicrofluidics, 2018. **12**(3): p. 034109.
51. Moore, T.L., et al., *Nanoparticle colloidal stability in cell culture media and impact on cellular interactions.* Chemical Society Reviews, 2015. **44**(17): p. 6287-6305.
52. Lewinski, N., V. Colvin, and R. Drezek, *Cytotoxicity of Nanoparticles.* Small, 2008. **4**(1): p. 26-49.
53. Nan, A., et al., *Cellular Uptake and Cytotoxicity of Silica Nanotubes.* Nano Letters, 2008. **8**(8): p. 2150-2154.
54. Ribeiro, L.N.d.M., et al., *Use of nanoparticle concentration as a tool to understand the structural properties of colloids.* Scientific Reports, 2018. **8**(1): p. 982.
55. De Jong, W.H. and P.J.A. Borm, *Drug delivery and nanoparticles: Applications and hazards.* International Journal of Nanomedicine, 2008. **3**(2): p. 133-149.

TOC

Christophoros Mannaris[1*], Chuanxu Yang[2], Dario Carugo[1,4], Joshua Owen[1], Jeong Yu Lee[1], Sandra Nwokeoha[1], Anjali Seth,[1], Boon Mian Teo[1,2,3*]

Title Acoustically Responsive Polydopamine Nanodroplets: A Novel Theranostic Agent

ToC

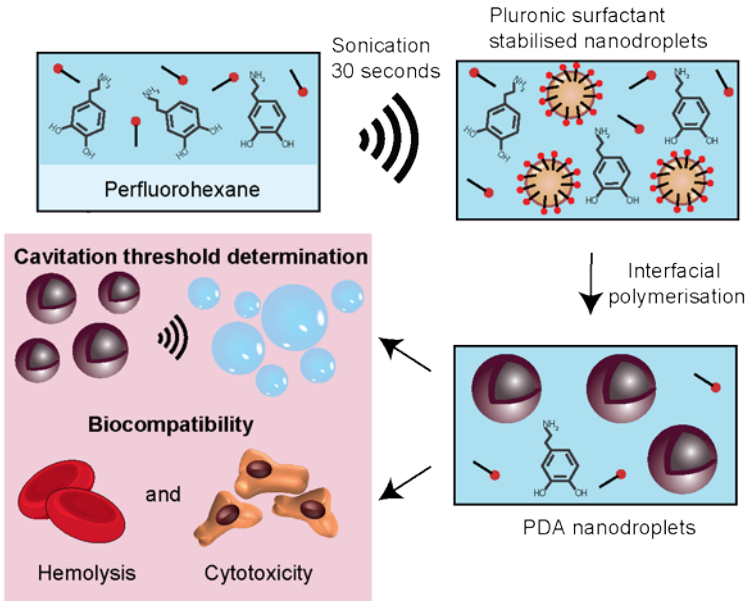

Supporting Information

Title Acoustically Responsive Polydopamine Nanodroplets: A Novel Theranostic Agent

Christophoros Mannaris[1*], Chuanxu Yang[2], Dario Carugo[1,4], Joshua Owen[1], Jeong Yu Lee[1], Sandra Nwokeoha[1], Anjali Seth,[1], Boon Mian Teo[1,2,3*]

Supporting information

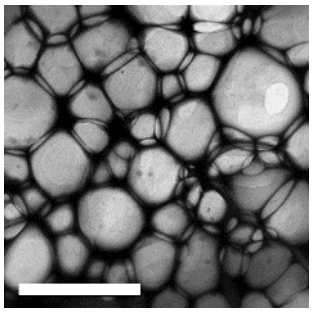

Figure S1. TEM images of microbubbles generated from vaporisation of PDA nanodroplets. Scale bar: 2 μm.

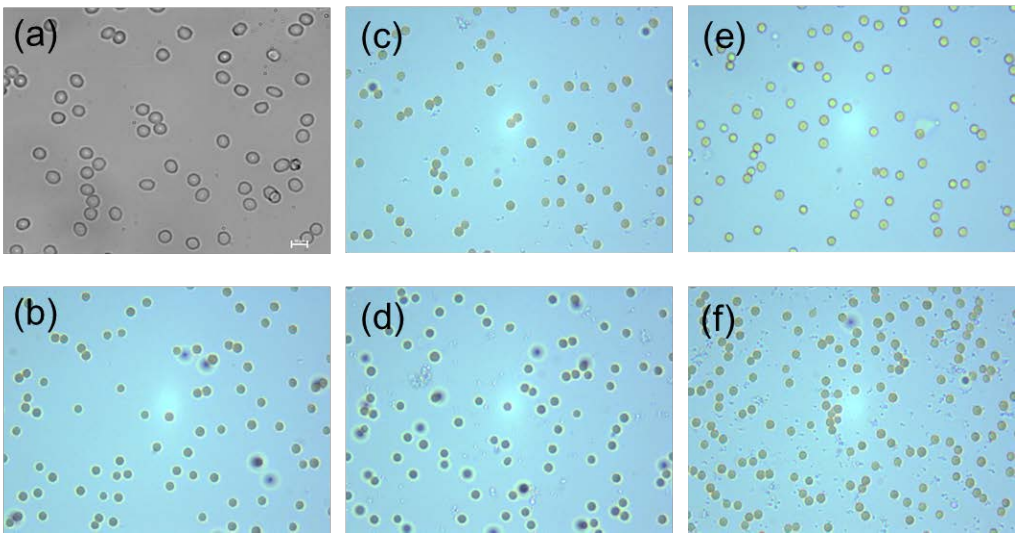

Figure S2. Optical images of red blood cells after incubation with increasing nanodroplets concentration: RBC in (a) PBS solution, (b) 1/32, (c) 1/16, (d) 1/8, (e) 1/4, (f) 1/2 fraction of nanodroplets concentration (original concentration of nanodroplets: $1x10^8$).